BBA - Molecular Basis of Disease 1866 (2020) 165622

Contents lists available at ScienceDirect

BBA - Molecular Basis of Disease

journal homepage: www.elsevier.com/locate/bbadis

In-depth phenotyping reveals common and novel disease symptoms in a hemizygous knock-in mouse model (*Mut*-ko/ki) of *mut*-type methylmalonic aciduria

Marie Lucienne[a,b,c], Juan Antonio Aguilar-Pimentel[d], Oana V. Amarie[d], Lore Becker[d], Julia Calzada-Wack[d], Patricia da Silva-Buttkus[d], Lillian Garrett[d,e], Sabine M. Hölter[d,e], Philipp Mayer-Kuckuk[d], Birgit Rathkolb[d,f,g], Jan Rozman[d,g], Nadine Spielmann[d], Irina Treise[d], Dirk H. Busch[h], Thomas Klopstock[g,i,j,k], Carsten Schmidt-Weber[l], Eckhard Wolf[f], Wolfgang Wurst[e,j,k,m], Merima Forny[a], Déborah Mathis[n], Ralph Fingerhut[o], D. Sean Froese[a,b], Valerie Gailus-Durner[d], Helmut Fuchs[d], Martin Hrabě de Angelis[d,g,p], Matthias R. Baumgartner[a,b,c,*]

[a] *Division of Metabolism and Children's Research Center, University Children's Hospital Zurich, Zurich, Switzerland*
[b] *radiz – Rare Disease Initiative Zurich, Clinical Research Priority Program for Rare Diseases, University of Zurich, Zurich, Switzerland*
[c] *Zurich Center for Integrative Human Physiology, University of Zurich, Zurich, Switzerland*
[d] *German Mouse Clinic, Institute of Experimental Genetics, Helmholtz Zentrum München, German Research Center for Environmental Health, Neuherberg, Germany*
[e] *Institute of Developmental Genetics, Helmholtz Zentrum München, German Research Center for Environmental Health, Neuherberg, Germany*
[f] *Institute of Molecular Animal Breeding and Biotechnology, Gene Center, Ludwig-Maximilians-University München, Munich, Germany*
[g] *German Center for Diabetes Research (DZD), Neuherberg, Germany*
[h] *Institute for Medical Microbiology, Immunology and Hygiene, Technical University of Munich, Trogerstrasse 30, 81675 Munich, Germany*
[i] *Department of Neurology, Friedrich-Baur-Institut, Ludwig-Maximilians-Universität München, Ziemssenstrasse 1a, 80336 Munich, Germany*
[j] *Deutsches Institut für Neurodegenerative Erkrankungen (DZNE) Site Munich, Schillerstrasse 44, 80336 Munich, Germany*
[k] *Munich Cluster for Systems Neurology (SyNergy), Adolf-Butenandt-Institut, Ludwig-Maximilians-Universität München, Schillerstrasse 44, 80336 Munich, Germany*
[l] *Center of Allergy & Environment (ZAUM), Technische Universität München, and Helmholtz Zentrum München, Neuherberg, Germany*
[m] *Chair of Developmental Genetics, Center of Life and Food Sciences Weihenstephan, Technische Universität München, c/o Helmholtz Zentrum München, Neuherberg, Germany*
[n] *Division of Clinical Chemistry and Biochemistry, University Children's Hospital Zurich, Switzerland*
[o] *Swiss Newborn Screening Laboratory, University Children's Hospital Zurich, Zurich, Switzerland*
[p] *Chair of Experimental Genetics, Center of Life and Food Sciences Weihenstephan, Technische Universität München, Freising-Weihenstephan, Germany*

ARTICLE INFO

Keywords:
Methylmalonic aciduria
Mouse model
Failure to thrive
Decreased cardiac function
Liver phenotype
Ovarian atrophy

ABSTRACT

Isolated methylmalonic aciduria (MMAuria) is primarily caused by deficiency of methylmalonyl-CoA mutase (MMUT or MUT). Biochemically, MUT deficiency results in the accumulation of methylmalonic acid (MMA), propionyl-carnitine (C3) and other metabolites. Patients often exhibit lethargy, failure to thrive and metabolic decompensation leading to coma or even death, with kidney and neurological impairment frequently identified in the long-term. Here, we report a hemizygous mouse model which combines a knock-in (ki) missense allele of *Mut* with a knock-out (ko) allele (*Mut*-ko/ki mice) that was fed a 51%-protein diet from day 12 of life, constituting a bespoke model of MMAuria. Under this diet, mutant mice developed a pronounced metabolic phenotype characterized by drastically increased blood levels of MMA and C3 compared to their littermate controls (*Mut*-ki/wt). With this bespoke mouse model, we performed a standardized phenotypic screen to assess the whole-body impairments associated with this strong metabolic condition. We found that *Mut*-ko/ki mice show common clinical manifestations of MMAuria, including pronounced failure to thrive, indications of mild neurological and kidney dysfunction, and degenerative morphological changes in the liver, along with less well described symptoms such as cardiovascular and hematological abnormalities. The analyses also reveal so far unknown disease characteristics, including low bone mineral density, anxiety-related behaviour and ovarian atrophy. This first phenotypic screening of a MMAuria mouse model confirms its relevance to human disease,

* Corresponding author at: Division of Metabolism and Children's Research Center, University Children's Hospital Zurich, Zurich, Switzerland.
E-mail address: Matthias.Baumgartner@kispi.uzh.ch (M.R. Baumgartner).

https://doi.org/10.1016/j.bbadis.2019.165622
Received 18 March 2019; Received in revised form 14 October 2019; Accepted 21 November 2019
Available online 23 November 2019

reveals new alterations associated with MUT deficiency, and suggests a series of quantifiable readouts that can be used to evaluate potential treatment strategies.

1. Introduction

Methylmalonic aciduria (MMAuria) is a rare autosomal recessive inborn error of metabolism caused by deficiency of the mitochondrial enzyme methylmalonyl-CoA mutase (MMUT or MUT) (OMIM entry *609058) [1]. The MUT enzyme catalyses the reversible isomerization of $_{L}$-methylmalonyl-CoA into succinyl-CoA, an intermediate in the tricarboxylic acid cycle, by using vitamin B_{12} (cobalamin, Cbl) in its cofactor form 5′-deoxyadenosylcobalamin (AdoCbl). In humans, this reaction represents an important step in propionate catabolism, funneling metabolites from the breakdown of branched-chain amino acids (valine, isoleucine, methionine, and threonine), odd-chain fatty acids, and the side chain of cholesterol into the tricarboxylic acid cycle [2]. Deficient activity of MUT results either from defects of the MUT apo-enzyme or from defects of intracellular synthesis of AdoCbl. Apo-enzyme defects are traditionally divided into *mut*^{0} and *mut*$^-$ classes on the basis of residual *in vitro* MUT activity, whereby patients classified as *mut*$^-$ retain some residual activity and are responsive *in vitro* to Cbl supplementation while *mut*^{0} are not [3,4]. This often translates into *mut*$^-$ patients presenting later with milder disease than *mut*^{0} [4,5]. Biochemically, MMAuria is characterized by the accumulation of metabolites, such as methylmalonic acid (MMA), propionylcarnitine (C3), and 2-methylcitrate in tissues and body fluids [5]. MMAuria patients often present in the newborn period with failure to thrive, lethargy, repeated vomiting and life-threatening metabolic decompensations. Most surviving patients develop chronic kidney damage, and many suffer from neurological deterioration. As a consequence, the risk of severe disability or death is very high [6]. Patients are often supplemented with carnitine and Cbl, and in order to reduce the throughput of the MUT pathway, a dietary restriction involving a low-protein intake is usually implemented [5,7,8].

To study the pathomechanisms of *mut*-type MMAuria, mouse models of disease have been utilized. Previously, two *Mut* knock-out (*Mut*-ko) mouse models have been generated, resulting in complete null mutants; however, most homozygous pups did not survive past 24 h [9,10]. To circumvent this lethality, in separate studies, adeno-associated virus delivery [11] and transgene expression [12] in the liver were introduced. A novel hemizygous mouse model of MMAuria was generated by Forny et al. [13], combining a knock-in (ki) allele with a ko allele (*Mut*-ko/ki), whereby the ki allele was based on the p.Met700Lys patient missense mutation (p.Met698Lys in mouse) [14]. Compared to their heterozygous littermate controls (*Mut*-ki/wt), *Mut*-ko/ki females showed increased blood and tissue levels of MMA and of C3 normalized to acetylcarnitine (C2), as well as failure to thrive and renal dysfunction. However, consistent with the *mut*$^-$ phenotype found in human patients carrying the p.Met700Lys mutation, this model recapitulated a milder version of the disease and a dietary strategy was applied to exacerbate the phenotype. Thereby, *Mut*-ko/ki mice were fed either a high-protein or precursor-enriched diet to increase the throughput of the MUT pathway. These interventions led to more overt signs of the disease, among which were very high levels of accumulating relevant metabolites in blood and tissues [13]. Nevertheless, the dietary-driven increase of the biochemical phenotype could only be shown acutely, as the mice lost weight too rapidly to continue beyond a few days.

To thoroughly investigate *in vivo* alterations associated with the metabolic impairment in MMAuria, one strategy is to perform a systemic phenotyping study that assesses all clinically relevant organ systems. The full screening approach based on standard protocols may uncover potential mutation-related abnormalities in the whole body in a reliable and reproducible manner, without introducing a researcher's bias as to which systems are expected to be affected [15]. To our knowledge, no mouse model of MMAuria has yet undergone such an unbiased phenotyping screen.

We have developed a new strategy of dietary challenge by feeding our mice with a 51%-protein diet from day 12 of life. In this way, *Mut*-ko/ki mice start accumulating metabolites at a very early age, akin to what is found clinically, but avoid rapid weight loss, enabling long-term investigation. Using this model, we have performed a broad phenotyping screen and found dysfunctions across many organ systems, many of which parallel clinical findings in patients with MMAuria. We have further identified new phenotypic traits that may form the basis of future clinical and molecular investigations.

2. Material and methods

2.1. Ethics statement

In Zurich, all animal experiments were approved by the legal authorities (license 048/2016; Kantonales Veterinäramt Zürich, Switzerland) and performed according to the legal and ethical requirements. In Munich, mice were maintained according to the German Mouse Clinic (GMC) housing conditions and German laws. All tests performed at the GMC were approved by the responsible authority of the district government of Upper Bavaria, Germany.

2.2. Animal housing

In Zurich, mice were bred and housed in single-ventilated cages with a 12:12 h light/dark cycle and an artificial light of approximately 40 Lux in the cage. The animals were kept under controlled humidity (45–55%) and temperature (21 ± 1 °C) and housed in a barrier-protected specific pathogen-free unit. Mice had *ad libitum* access to sterilized drinking water and to pelleted and extruded mouse diet. All parameters were monitored continuously. To generate the experimental *Mut*-ko/ki and the control *Mut*-ki/wt mice, *Mut*-ko/wt females were crossed with *Mut*-ki/ki males. In Munich, animal housing was performed in strict accordance with directive 2010/63/EU. Mice were housed in individually ventilated caging (IVC) systems operating with positive pressure (Sealsafe plus, GM 500, Tecniplast, Buggugiate, Italy) under specific pathogen-free conditions. All mice received autoclaved wood chips (Lignocel select fine, J. Rettenmaier & Soehne GmbH, Rosenberg, Germany) and paper stripes (Arbocel crinclets natural Rettenmaier & Soehne GmbH) as bedding and nesting material, irradiated protein rich diet (51%) for rodents (optimized prior to this study, for details see below) and sterile-filtered tap water *ad libitum*. Light was adjusted to a 12:12 h light/dark cycle with a 10 min period of dimmed light to simulate sunrise/sunset.

2.3. Diet studies

For the optimization of the dietary conditions, mice were fed with several types of high-protein diets (51%, 42% and 33% of protein) and a reference diet (18% of protein, diet U8978 version 22). All the diets were manufactured by Safe and the composition of the high-protein diets was based on the reference diet. Mouse monitoring entailed regular weight measurements and blood collections from tail vein.

2.4. Metabolite measurements

Thirty microlitres of blood was collected from tail vein and put on a

filter card. Whole blood concentration of MMA, acetylcarnitine and propionylcarnitine was determined on dried blood spots, as previously described [13]. Measurements were performed in duplicates and averages were calculated prior to data analysis.

Plasma was prepared by collecting ~50 μL of blood from tail vein in a tube coated with K_2-EDTA before centrifugation at 1500*g* for 10 min. Determination of MMA concentration: Plasma and urine samples (~20 μL and ~70 μL respectively) were analyzed by liquid chromatography mass spectrometry (LC-MS/MS) on a Thermo Scientific UltiMate 3000 Rapid Separation LC coupled to an AB Sciex 5500 TripleQuad mass spectrometer using a commercial kit (Recipe ClinMass® advanced). Plasma and urine samples were first diluted with water (factor 2 and 20 for control plasma and urine respectively, and factor 500 and 50′000 for mutant plasma and urine respectively), to which internal standard (d3-MMA) was added. The samples were vortexed, centrifuged, the supernatant transferred to HPLC vials, and 2 μL were injected into the instrument. Creatinine was determined by enzymatic assay on a routine analyzer Alinity c from Abbott Laboratories.

2.5. Blood gases measurements

Blood was collected from tail vein and analyzed immediately for determination of pH, pCO_2 and HCO_3^- on a Radiometer ABL 800 blood gas analyzer.

2.6. B12 treatment

Mice were administrated 50 μg/g hydroxocobalamin daily over 50 days, starting at 2 months of age, given intraperitoneally. After one week of treatment, mice were switched to a 51%-protein diet.

2.7. Phenotypic screening

At the GMC, 30 mutant mice (15 females and 15 males) and 26 controls (14 females and 12 males) were subjected to an extensive phenotypic screening, including standardized phenotyping in the areas of dysmorphology, behaviour, neurology, nociception, energy metabolism, clinical chemistry, cardiovascular features, eye, immunology, and pathology [16] (see also www.mouseclinic.de). The phenotypic tests were part of the GMC screen and were performed according to standardized protocols as described [17–19]. The test pipeline started at the age of 10 weeks. Dependent of the test performed, animal number may vary, and is indicated in the figure/table.

2.8. Statistical analysis

In Zurich, the data analysis was performed using Graph Pad (version 8.0.0) and automated R-scripts (version 3.5.1). In Munich, unless otherwise indicated, the data generated by the GMC was analyzed using R (version 3.2.3). Tests for genotype effects were made by using *t*-test, Wilcoxon rank sum tests, linear models, or ANOVA and posthoc tests, or Fisher's exact test depending on the assumed distribution of the parameter and the questions addressed to the data. A p-value < 0.05 has been used as level of significance; a correction for multiple testing has not been performed (about 500 parameters belonging to 14 different disease areas are measured during the primary screening).

3. Results

3.1. Optimization of dietary challenge

We previously showed that a switch to a high-protein diet (60%-protein) at approximately day 60 of life triggers a significant increase in metabolite levels in *Mut*-ko/ki mice [13]. Unfortunately, this is accompanied by drastic weight loss requiring the mice to be sacrificed after 4 days. Based on these data, we attempted a new strategy of dietary challenge. We fed 6-week-old *Mut*-ko/ki females with a protein-content diet of 51%, 42% and 33%-protein chow that were isocaloric to each other and with a reference chow (16%-protein). As might be expected, a protein-content dependent effect was observed in detection of

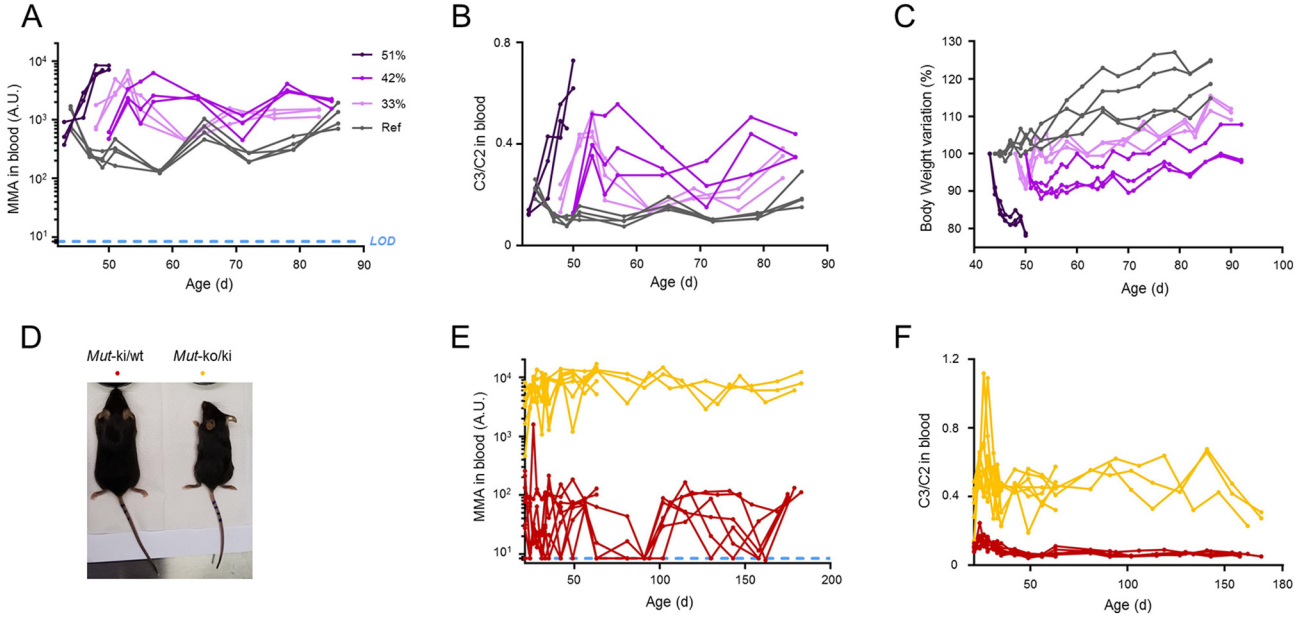

Fig. 1. *Mut*-ko/ki mice exhibit drastically elevated metabolite levels and failure to thrive under a 51%-protein diet. Panels (A)–(B): Impact of high-protein diet initiated in older (~6-week-old) *Mut*-ko/ki females. Percentages given represent protein composition in diet (Ref: reference chow, 16%-protein). Measurement of (A) detectable methylmalonic acid (MMA) in arbitrary units (A.U.) and (B) propionylcarnitine (C3) normalized to acetylcarnitine (C2) in dried blood spots. (C) Change in body weight after switching to a high-protein diet, with body weight on the day the high-protein diet was introduced taken as 100%. For A–C: Each tracked point represents a single mouse. The diet shown was provided immediately after the first data point. Panels D–F: Impact of 51% protein diet given in younger (12-day-old) females. (D). Evidence of growth delay in a 19-week-old female *Mut*-ko/ki mouse compared to her *Mut*-ki/wt (littermate) sister. Measurement of (E) MMA and (F) C3 normalized to C2 in dried blood spots over the first 6 months of life. Each tracked point represents a single mouse. *LOD*: limit of detection.

MMA (Fig. 1A) and C3 normalized to C2 (Fig. 1B) detected in dried blood spots, whereby the 51%-protein diet led to the strongest increase in biochemical parameters. However, *Mut*-ko/ki mice challenged with a 51%-protein diet unfortunately also displayed drastic weight loss (Fig. 1C). We hypothesized that this was due to a sudden reduction in food intake, linked to the switch to a different type of food and pellet texture (unpublished observations and [20]). To circumvent this dietary change, we supplied mice with the 51%-protein pellets starting from day 12 of life, ensuring that from weaning it was the only solid food available. By this method, although *Mut*-ko/ki mice were smaller than their littermates (Fig. 1D), we no longer detected sudden weight loss (Fig. S1), enabling long-term studies. An initial cohort of female mice on this diet, observed for almost six months, retained persistently elevated metabolite levels (Fig. 1E and F), suggesting this was a suitable strategy.

3.2. A biochemically relevant bespoke mouse model

Using the *Mut*-ko/ki mice (or *Mut*-ki/wt littermate controls) on a 51% protein diet from day 12 of life, our bespoke model, we investigated larger cohorts of mice including both sexes. The massive elevations in metabolic parameters presented in Fig. 1 were confirmed in cohorts of up to 15 mice per genotype per sex for both MMA (Fig. 2A) and C3/C2 (Fig. 2B) at both 5 and 20 weeks of age. On average, *Mut*-ko/ki males and females showed an ~100-fold increase in MMA levels and ~4-fold increase in C3/C2 compared to their littermates and both parameters were stable over time (Fig. 2A and B). This corresponds to an approximate 15-fold increase in MMA and 3-fold increase in C3/C2 compared to *Mut*-ko/ki mice on a reference diet (compare Fig. 1A and B with Fig. 2A and B). The physiological relevance of these elevations were confirmed in a cohort of female mice whereby *Mut*-ko/ki mice had plasma MMA ranging from 100 to 1000 μM, while urinary MMA was in the range of 10–100 mol/mol creatinine, concentrations which are ~100-fold higher than their littermate controls (Fig. 2C and D). Since some *mut*$^{-}$ patients are treated with intramuscular injection of Cbl, we further performed daily intraperitoneal hydroxocobalamin injections in *Mut*-ko/ki females raised on normal chow and switched to a 51%-protein diet seven days after the start of injections. These mice showed a reduction in MMA levels compared to sham treated mice (injected with NaCl) over seven weeks of time (Fig. S2), indicating they were partially amenable to Cbl treatment.

In order to determine which further clinically translatable disease aspects are present in these mice, we performed a full standardized phenotyping of our bespoke MMAuria mouse model, completed as part of the mandate of the German Mouse Clinic (GMC) to characterize mouse models of human disease [15,16,21]; https://www.mouseclinic.de). In accordance with our optimized protocol, for further studies *Mut*-ko/ki and *Mut*-ki/wt mice were challenged with a 51%-protein diet from day 12 of life. Cohorts of 15 mice per sex/genotype were used for in-depth phenotyping. Although 60 mice were generated, 4 were excluded from the final analysis - 1 *Mut*-ki/wt female died after the first test, and 3 *Mut*-ki/wt males had very low body mass combined with extremely high liver enzyme activities, suggesting that they suffered from chronic liver disease, which was confirmed upon autopsy.

3.3. Confirmation that Mut-ko/ki mice show failure to thrive

The first and most obvious phenotypic finding in the *Mut*-ko/ki mice was that of growth delay in both males and females (Fig. 3A and B), consistent with observations in our initial cohort (Figs. 1D and S1). *Mut*-ko/ki mice of both sexes were considerably lighter than their heterozygous littermate controls at time of first weighing (approx. day 24 of life), a difference that was further exaggerated over the following 4 weeks (Fig. 3A and B). After approximately day 70 of life *Mut*-ko/ki mice showed similar growth curves to their littermates. Nevertheless, they remained underweight. To identify whether their reduced growth was associated with decreased food and water intake, these parameters were measured over a period of 21 h, starting 5 h before lights-off in the evening. Over this time, *Mut*-ko/ki mice ate and drank less than their littermates (Fig. 3C and D). When adjusted for the body weight difference, food and water consumption did not differ between genotypes.

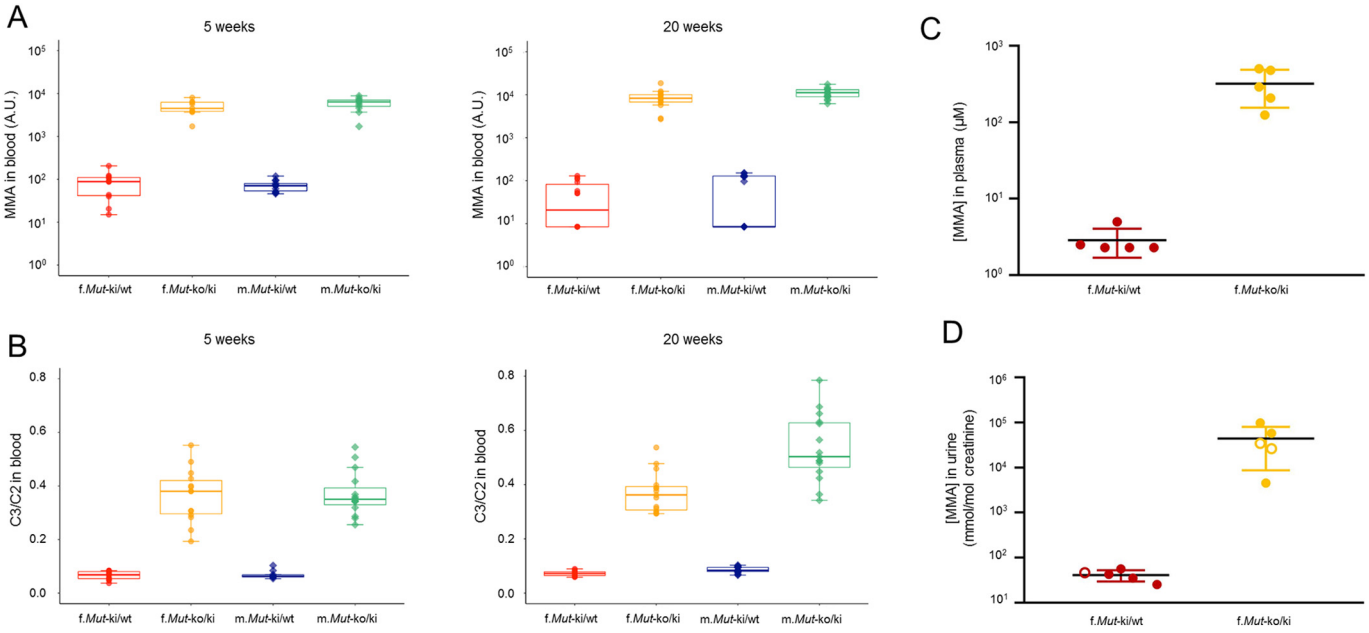

Fig. 2. Impact of 51% protein diet initiated at a younger age (12-day-old) in large cohorts of both sexes. Measurement of methylmalonic acid (MMA) in dried blood spots in (A) 5-week-old and 20-week-old mice. Measurement of propionylcarnitine (C3) normalized to acetylcarnitine (C2) in dried blood in (B) 5-week-old and 20-week-old mice. $p < 0.0001$. Significant difference determined by Wilcoxon Mann Whitney Tests using automated R-scripts (version 3.5.1). C-D: MMA concentrations in plasma (C) and urine (D) in 5 *Mut*-ki/wt and 5 *Mut*-ko/ki female mice. Urine MMA was normalized to simultaneous urine creatinine from each sample (closed circles) or average creatinine from all samples (open circles).

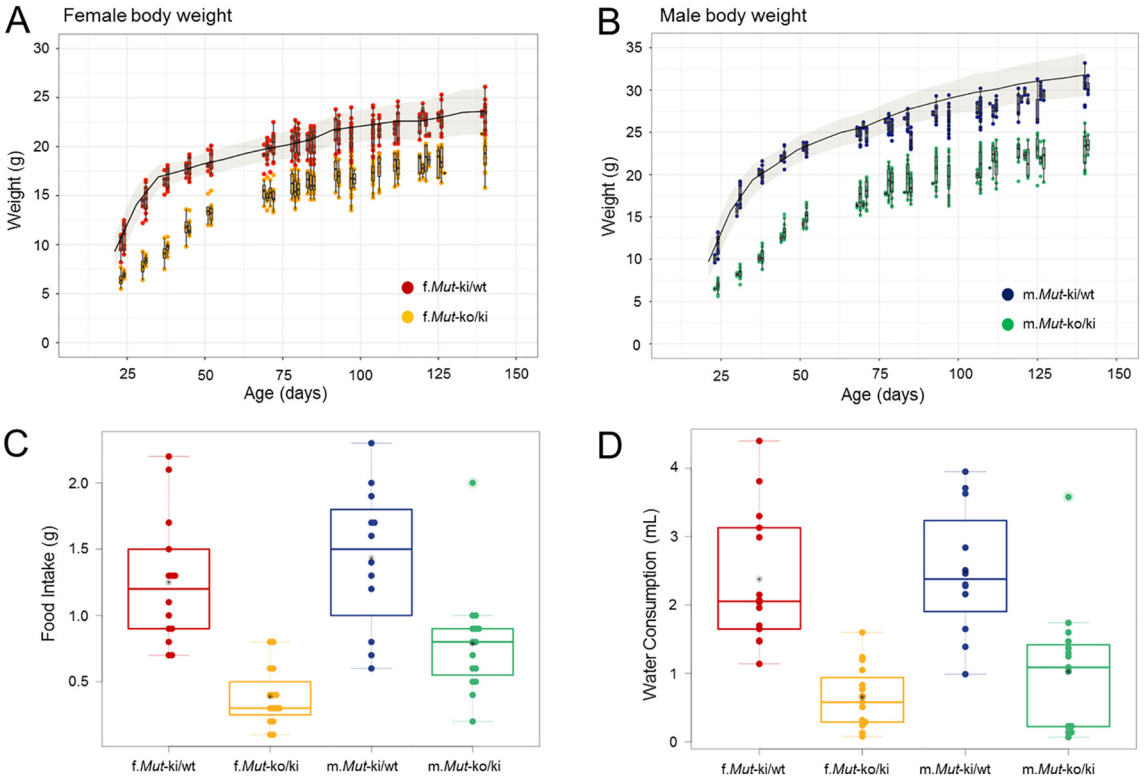

Fig. 3. Impact of optimized dietary strategy on growth, food intake and water consumption. Evidence of growth delay in *Mut*-ko/ki females (A) and *Mut*-ko/ki males (B) compared to *Mut*-ki/wt littermate controls of each sex over 4 months of life (n ≥ 12 for each). Growth of wild-type C57BL/6J mice fed with a normal diet (19.3% protein) is shown as mean (black line) ± 1 S.D. (grey shading) for each sex (data from The Jackson Laboratory, https://www.jax.org/jax-mice-and-services/strain-data-sheet-pages/body-weight-chart-000664). Monitoring of food intake (C) and water consumption (D) over 21 h at the age of 14 weeks. Each point represents a single mouse.

3.4. Along with smaller size, Mut-ko/ki mice show bone alterations

Consistent with reduced weight, we found in our initial cohort that *Mut*-ko/ki females appeared smaller than their littermates (Fig. 1D). In this larger cohort, we found that their decreased stature corresponded to decreased tibia length (females 17.69 [16.8, 17.72] mm in *Mut*-ko/ki *versus* 18.42 [18.14, 18.64] mm in *Mut*-ki/wt, p-value < 0.05; males (17.94 [17.89, 18.02] mm in *Mut*-ko/ki *versus* 18.36 [18.29, 18.71] mm in *Mut*-ki/wt, p-value < 0.05; median [first quartile, third quartile], p-values by Wilcoxon rank-sum test:). Using dual-energy X-ray absorptiometry (DEXA) analysis of both the whole skeleton (excluding the head) and lumbar spine, we found bone area and bone mineral content (BMC) to be decreased when males and females were combined (Table 1) or evaluated separately (Tables S1 and S2). As the magnitude of BMC reduction was greater than the decrease in bone area, decreased bone mineral density (BMD) was identified in these mice (Table 1). Therefore, *Mut*-ko/ki mice have shorter and less dense bones than their littermates. These changes were not due to chronic exposure to metabolic acidosis, since blood pH, pCO_2 and bicarbonate were not found to be changed in selected female mice under the same dietary conditions (Fig. S3). We further found that *Mut*-ko/ki males and females had reduced grip strength using only two paws or with all four paws. However, regression analysis indicated that this strongly corresponded to their decreased body weight (Fig. S4). Therefore, muscle function does not appear to be primarily affected by the defect.

3.5. Mut-ko/ki mice display hypoactivity and anxiety-related behaviour

We further performed an examination of behavioural and neurological related changes. Using an open field test, *Mut*-ko/ki males and females had decreased exploratory behaviour, as they spent less time (Figs. 4A and S5A) and had reduced distance (Figs. 4B and S5B) in the

Table 1
DEXA analysis of whole mouse and region-specific bone mineral density and content.

	Mut-ki/wt (n = 26)	*Mut*-ko/ki (n = 30)	Δ% ((*Mut*-ko/ki - *Mut*-ki/wt)/*Mut*-ki/wt)	ANOVA genotype p-value
Total weight whole mouse DEXA [g]	24.0 ± 3.7	18.8 ± 2.5	−21.7	< 0.001
Bone area whole mouse [cm^2]	8.67 ± 0.62	7.45 ± 0.45	−14.1	< 0.001
BMC whole mouse [mg]	554.820 ± 76.149	412.151 ± 48.226	−25.7	< 0.001
BMD whole mouse [mg/cm^2]	63.7 ± 4.1	55.1 ± 3.5	−13.5	< 0.001
Bone area ROI [cm^2]	0.47 ± 0.03	0.41 ± 0.03	−12.8	< 0.001
BMC ROI [mg]	33.823 ± 4.304	24.038 ± 3.519	−28.9	< 0.001
BMD ROI [mg/cm^2]	72.5 ± 6.4	58.2 ± 5.1	−19.7	< 0.001

For each genotype male and female mice were pooled. Data provided as group means ± standard deviation and ANOVA (Tukey multiple comparisons of means). BMC: bone mineral content; BMD: bone mineral density; ROI: region of interest.

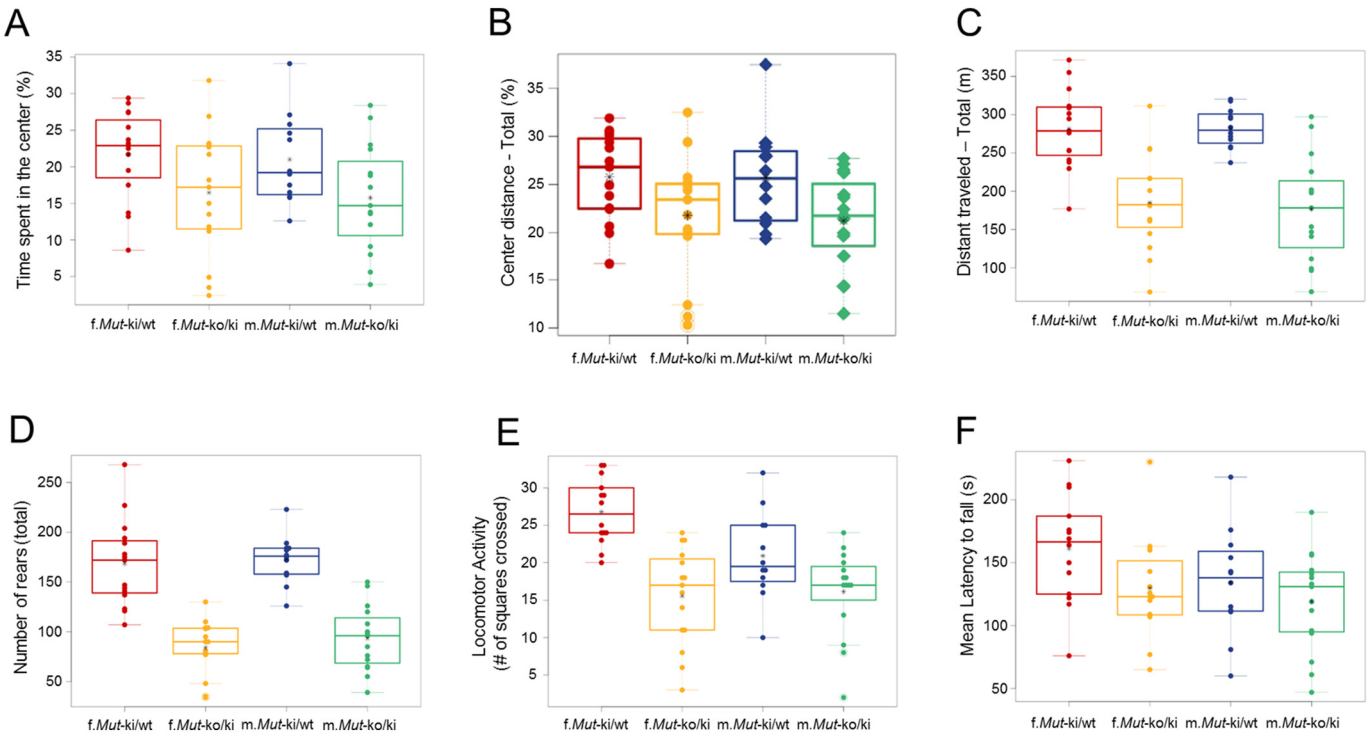

Fig. 4. *Mut*-ko/ki mice are hypoactive and show anxiety-related behaviour compared to *Mut*-ki/wt. In an open field test used as a novel environment (20 min test duration), evidence of decreased percent permanence time spent in the center, p-value 0.009 (A) and percent distance spent in the center, p-value 0.004 (B), decreased distance travelled, p-value < 0.001 (C), and decreased number of rears, p-value < 0.001 (D). During the SHIRPA test (30 s), evidence of reduced locomotor activity, p-value < 0.001 (E). The rotarod revealed slightly reduced latencies to fall in *Mut*-ko/ki males and females, p-value 0.034 (F).

centre of the arena, consistent with anxiety-related behaviour. The open field test also revealed a clear decrease in locomotor and exploratory activities, as indexed by a diminution in the total distance travelled (Figs. 4C and S5C) and total rearing activities (Figs. 4D and S5D), which was corroborated using a modified SHIRPA protocol (Fig. 4E). This hypoactivity was accompanied by a reduced locomotor speed in the open field (Table S3) and a shorter latency to fall in the rotarod test, this latter indicating a potential decrease in motor coordination and balance (Fig. 4F). In contrast to these acute tests in a novel environment, when measured over 21 h in an environment close to home cage conditions, we did not observe any difference in average distance or rearing between *Mut*-ko/ki and *Mut*-ki/wt mice (Table S4), although we note the variability between mice in these longer-term tests. In sum, these findings support a hypothesis that *Mut*-ko/ki mice are anxious and hypoactive, at least when exposed to novel environments.

3.6. Decreased thermal sensitivity

We evaluated the thermal sensitivity of *Mut*-ko/ki and *Mut*-ki/wt mice using a hotplate assay. We found that both the first (Fig. 5A) and second (Fig. 5B) reactions of the *Mut*-ko/ki mice were retarded compared to their littermates. However, the types of reactions (first hind paw shaking, then licking) were not different (data not shown). These retarded hotplate reactions may indicate hypoalgesia.

3.7. Further neurological findings

Further neurology and behaviour tests did not identify any major differences between *Mut*-ko/ki and *Mut*-ki/wt mice. Apart from decreased locomotor activity, all observation parameters, part of the SHIRPA protocol, including tremor, transfer arousal, gait, *etc*. were not significantly different between the two groups (Table S5). We also did not identify specific deficiencies of vision, with the caveat that axial

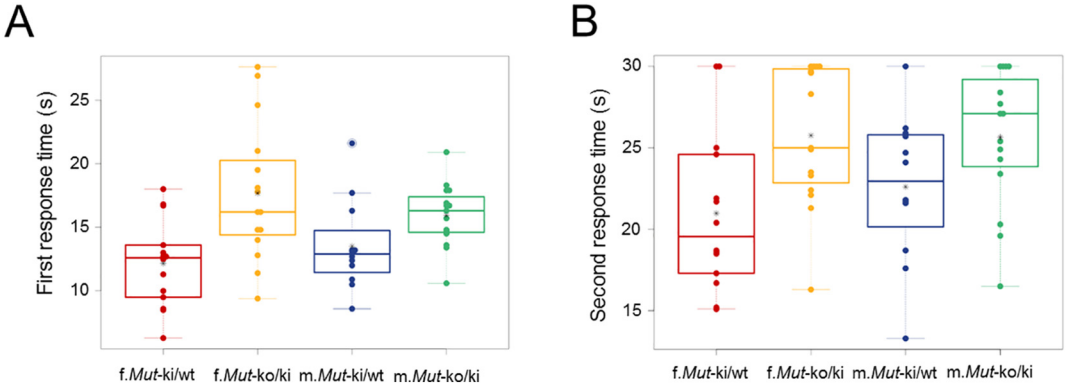

Fig. 5. *Mut*-ko/ki mice show a decreased thermal sensitivity. First (A) and second (B) reactions to the hotplate (p-value < 0.001 and p-value 0.002 respectively).

length and lens thickness were slightly decreased in some *Mut*-ko/ki mice (Fig. S6 and Table S6). Finally, we did not find specific hearing deficiencies as determined by acoustic startle (Table S7) and auditory brain response (Fig. S7) tests.

3.8. Evidence of early mild kidney dysfunction

In previous studies, electrolytes were found to be altered in *Mut*-ko/ki mice, suggestive of kidney dysfunction [13]. Here we found increased plasma levels of sodium, chloride and inorganic phosphate along with decreased total protein and alpha-amylase levels in *Mut*-ko/ki mice of either sex, while urea levels were increased in females only (Table 2). Nevertheless, our bespoke mouse model did not show any changes in plasma levels of calcium, potassium, creatinine, albumin and lactate dehydrogenase (Table 2). Standard hematoxylin and eosin staining in 20-week-old mice did not reveal any histological alterations in the kidney (Fig. S8).

3.9. Mut-ko/ki mice show signs of decreased cardiac function and hematological alterations

Awake electrocardiography and echocardiography recordings were performed in *Mut*-ko/ki and *Mut*-ki/wt mice to investigate the heart. Echocardiography identified a decrease in cardiac output (Fig. 6A), with no morphological or functional alterations noted (Tables S8 and S9). However, electrocardiography revealed a decreased heart rate and a concurrently increased RR length (Fig. 6B and Table S9). Furthermore, QT duration (Fig. 6C) and QT corrected for heart rate (QTc, Fig. 6D) were increased in the mutant male cohort. Both QT and QTc were also initially identified to be increased in the female mutant cohort, however, following removal of a single outlier, they were found to be unchanged (Fig. 6C and D). Histological investigation by hematoxylin and eosin staining did not identify any changes (Fig. S9).

Hematological investigations further indicated mild macrocytic anemia, as red blood cell counts, hemoglobin and hematocrit were all slightly decreased while mean cell volume and cellular hemoglobin content were increased in mutant mice (Table 3). These findings were associated with a decrease in plasma iron (Fig. 7A), as well as calculated total iron binding capacity (Fig. 7B) and transferrin saturation (Fig. 7C) in *Mut*-ko/ki mice. Further, there was evidence of thrombocytopenia as platelet counts and plateletcrit were decreased. Although platelet distribution width and mean platelet volume were not significantly altered, the proportion of large platelets (PLCR) was slightly reduced, predominantly in females (Table 3).

Total white blood cell counts, in contrast, were increased in *Mut*-ko/ki compared to controls (Table 3), which is in contradiction to what is observed in patients [5]. Increased white blood cell counts are consistent with the slightly elevated tumor necrosis factor alpha levels found in plasma (Fig. S10A). However, individual leukocyte populations were similar between *Mut*-ko/ki and *Mut*-ki/wt mice, whereby *Mut*-ko/ki females had slightly decreased granulocyte and decreased natural killer but increased natural killer T cell populations (Table S10). Likewise, plasma interleukin 6 (Fig. S10B) was not changed in the mutant mice and immunoglobulins, were within the normal range, although the concentration of IgA in *Mut*-ko/ki mice was marginally higher than in *Mut*-ki/wt mice (Table S11).

3.10. Alterations in the ovaries of Mut-ko/ki females

Histological investigations in ovaries of *Mut*-ko/ki females at the age of 20 weeks revealed an ovarian atrophy consisting of predominance of cords of pale stained hyperplastic interstitial tissue with fewer follicles with 100% penetrance (5 out of 5) compared to the control group (0 out of 5) (Fig. 8A and B). Histology of the testes, epididymis, funiculus spermaticus, prostrate, male accessory glands, uterus and vagina did not reveal any significant difference between *Mut*-ko/ki and their heterozygous littermate controls (data not shown).

3.11. Alterations in the liver of Mut-ko/ki mice

Mutant mice had a hepatocellular hypertrophy compared to control mice (Fig. 9). The hepatocellular hypertrophy comprised of enlarged hepatocytes tinctorially distinct and granular cytoplasm. High variation in the size of the cell nucleus (anisonucleosis) was also present as well as a high number of binucleated forms and a high rate of intranuclear inclusions in the liver of *Mut*-ko/ki mutant mice compared to controls.

4. Discussion

4.1. Establishment of a clinically relevant MMAuria mouse model

In this study, we established an optimized dietary strategy to challenge our MMAuria mouse model with a 51%-protein diet from day 12 of life. Compared to their littermates or the same mice on reference chow, this bespoke mouse model displays a pronounced metabolic phenotype characterized by elevated metabolite levels in blood, similar to patient levels. Correspondingly, according to published algorithms used for newborn screening, *Mut*-ko/ki and *Mut*-ki/wt mice would be correctly diagnosed as disease positive and negative respectively [22]. We also found that MMA concentrations in *Mut*-ko/ki mice challenged with a high-protein diet were responsive to Cbl treatment, suggesting that these mice are an excellent model to test novel treatments against

Table 2
Alterations of *Mut*-ko/ki plasma clinical chemistry measures.

	Females		Males		p-Value		
	Mut-ki/wt (n = 14)	Mut-ko/ki (n = 15)	Mut-ki/wt (n = 12)	Mut-ko/ki (n = 15)	Sex	Genotype	Sex:genotype
Sodium [mmol/l]	153 ± 2	156 ± 4	153 ± 2a	156 ± 4	0.924	0.005	0.986
Potassium [mmol/l]	4.4 ± 0.6	4.3 ± 0.7	3.8 ± 0.3a	4.2 ± 0.5	0.028	0.366	0.15
Chloride [mmol/l]	113.1 ± 2.1	115.2 ± 2.7	113.4 ± 2.2a	114.4 ± 2.9	0.744	0.028	0.431
Total protein [g/l]	47.7 ± 1.6	44 ± 2.2	47.9 ± 1.5	45.5 ± 1.9	0.087	< 0.001	0.173
Albumin [g/l]	24.3 ± 1.4	23.2 ± 1.1	23.6 ± 1.2	23.9 ± 1.1	0.967	0.187	0.04
Creatinine enz. [µmol/l]	12.83 ± 2.69	13.2 ± 3.54	12.06 ± 1.48	11.24 ± 2.99	0.079	0.766	0.437
Urea [mmol/l]	17.91 ± 2.36	22.85 ± 1.34	22.09 ± 2.48	22 ± 1.88	0.003	< 0.001	< 0.001
alpha-Amylase [U/l]	518.06 ± 42.53	424.62 ± 49.28	662.57 ± 55.66	506.68 ± 43.67	< 0.001	< 0.001	0.018
LDH [U/l]	169.2 ± 47.9	167.3 ± 37	142.7 ± 59.8	190.1 ± 105.8	0.921	0.222	0.187
Calcium [mmol/l]	2.21 ± 0.08	2.21 ± 0.08	2.18 ± 0.04	2.22 ± 0.08	0.466	0.344	0.245
Inorganic phosphate [mmol/l]	2.9 ± 0.46	3.57 ± 0.83	3.01 ± 0.3	3.42 ± 0.79	0.907	0.003	0.45

Data provided as mean ± sd. Genotype p-value was calculated by a linear model.
Plasma levels in *ad libitum* fed *Mut*-ko/ki and *Mut*-ki/wt mice. LDH: Lactate Dehydrogenase.

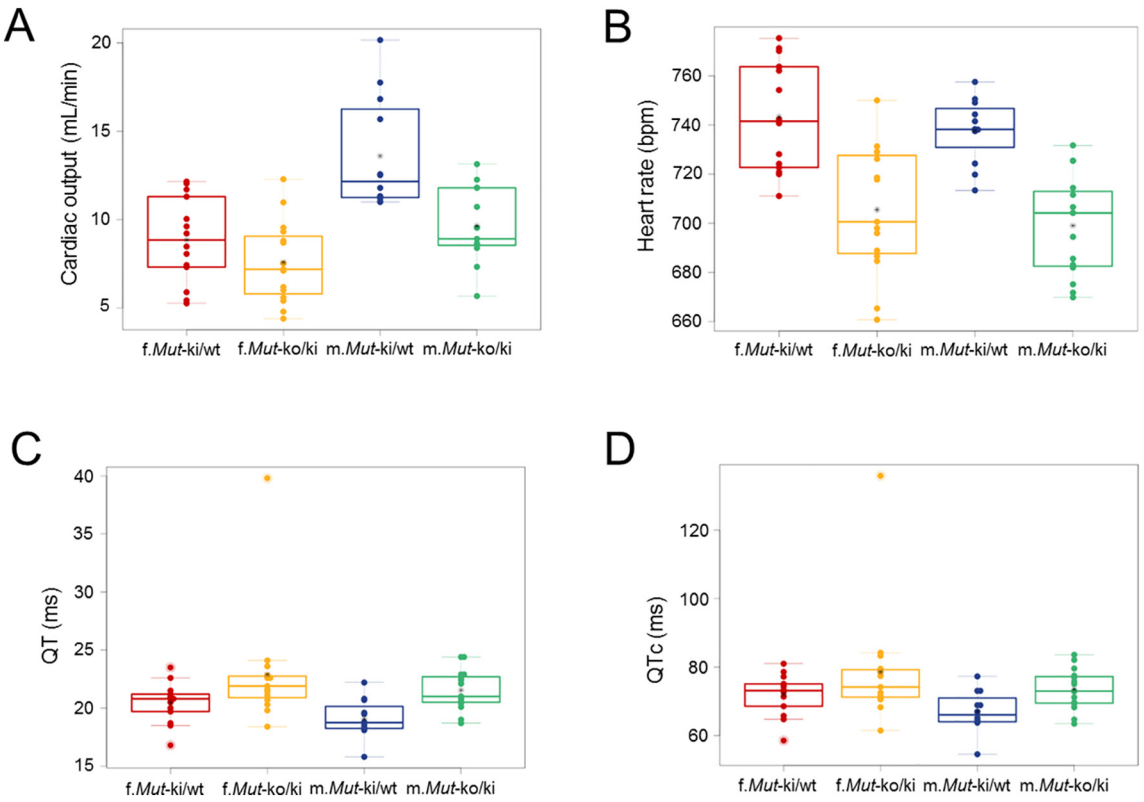

Fig. 6. *Mut*-ko/ki mice show decreased cardiac function. Echocardiography: evidence of decreased cardiac output, overall p-value both genders 0.01 (A). Electrocardiography: evidence of decreased heart rate, p-value females 0.001, p-value males < 0.001 (B), increased QT p-value females 0.032, p-value males 0.001 (C) and increased heart-rate corrected QT (QTc) p-value females 0.354, p-value males 0.015 (D).

MMAuria. It also suggests that patients harbouring the missense mutation p.Met700Lys, the equivalent mutation to the mouse p.Met698Lys in our *Mut*-ko/ki model, may be responsive to high dose parenteral vitamin B_{12} treatment *in vivo*.

In addition to elevated metabolite levels, we also found signs of common clinical manifestations of disease. The most prominent one, growth delay accompanied by decreased feeding and drinking, is akin to failure to thrive in patients. In MMAuria failure to thrive is one of the most prominent clinical findings in the first months to years of life and may be the revealing sign in patients that have not been diagnosed through a neonatal metabolic crisis or by newborn screening programs. In our mice, this failure to thrive is possibly related to the hypoactivity we also identified and may be due to complex multi-organ metabolic interactions, which are worth investigating further. We further observed a mild kidney impairment, characterized by small changes in electrolytes but no histological changes. These findings may be suggestive of early mild and likely pre-clinical kidney alterations in the *Mut*-ko/ki mice, with the potential of progression over time. In patients, renal complications are common in the course of the disease, with 47% presenting with chronic kidney disease by 6 years, and 12–14% with

Table 3
Hematological findings.

	Females		Males		p-Value		
	Mut-ki/wt (n = 14)	*Mut*-ko/ki (n = 15)	*Mut*-ki/wt (n = 12)	*Mut*-ko/ki (n = 15)	Sex	Genotype	Sex:genotype
RBC [Mio/mm^3]	11.57 ± 0.57	10.83 ± 0.64	11.43 ± 0.69	10.89 ± 0.56	0.812	< 0.001	0.531
HGB [g/dl]	18.41 ± 0.96	17.53 ± 0.89	17.82 ± 0.92	17.27 ± 0.96	0.092	0.006	0.502
HCT [%]	56.16 ± 2.53	54.19 ± 3.06	54.44 ± 2.94	53.75 ± 2.07	0.139	0.069	0.374
MCV [fl]	48.5 ± 0.65	50.13 ± 0.74	47.75 ± 0.75	49.47 ± 0.99	0.002	< 0.001	0.847
MCH [pg]	15.91 ± 0.32	16.2 ± 0.35	15.6 ± 0.49	15.87 ± 0.34	0.002	0.008	0.897
MCHC [g/dl]	32.79 ± 0.54	32.37 ± 0.81	32.73 ± 0.52	32.12 ± 0.75	0.414	0.006	0.595
RDW [%]	13.04 ± 0.41	12.99 ± 0.36	13.61 ± 0.59	13.63 ± 0.73	< 0.001	0.916	0.818
WBC [103/mm^3]	10.29 ± 2.87	15.58 ± 4.88	11.1 ± 2.33	12.51 ± 3.15	0.234	0.001	0.044
PLT [103/mm^3]	910 ± 147	792.93 ± 82.79	1067.58 ± 115.2	882.73 ± 107.92	< 0.001	< 0.001	0.277
MPV [fl]	6.28 ± 0.12	6.17 ± 0.13	6.26 ± 0.09	6.28 ± 0.12	0.179	0.193	0.051
PDW [fL]	5.54 ± 0.17	5.45 ± 0.26	5.55 ± 0.07	5.49 ± 0.12	0.612	0.09	0.723
PLCR [%]	2.43 ± 0.55	1.87 ± 0.52	2.33 ± 0.33	2.17 ± 0.4	0.432	0.006	0.11
PCT [%]	0.57 ± 0.09	0.49 ± 0.04	0.67 ± 0.07	0.55 ± 0.07	< 0.001	< 0.001	0.414

Values measured in EDTA-blood samples. Data provided as mean ± sd. All *p*-values calculated by a linear model. RBC: red blood cell count, HGB: hemoglobin, HCT: hematocrit, MCV: mean corpuscular volume, MCH: mean corpuscular hemoglobin, MCHC: mean corpuscular hemoglobin concentration, RDW: red blood cell distribution width, WBC: white blood cell, PLT: platelet count, MPV: mean platelet volume, PDW: platelet distribution width, PLCR: platelet large cell ratio, PCT: plateletcrit.

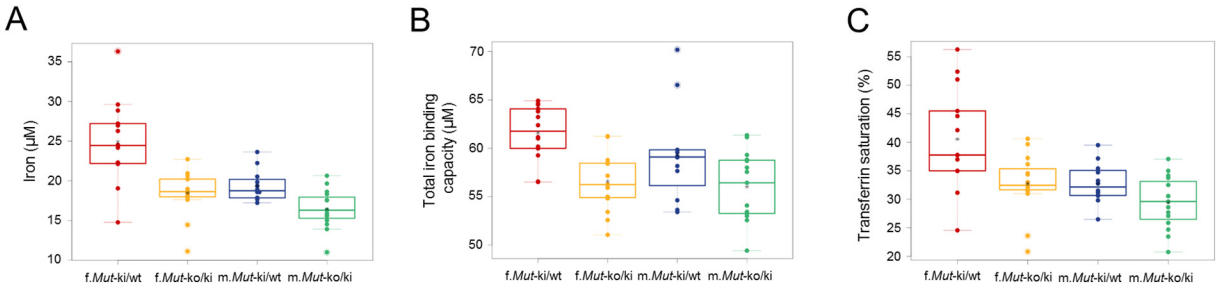

Fig. 7. *Mut*-ko/ki mice show hematological alterations. Plasma levels of iron, p-value < 0.001 (A), total iron binding capacity, p-value < 0.001 (B) and calculated transferrin saturation, p-value 0.001 (C) in *ad libitum* fed *Mut*-ko/ki and *Mut*-ki/wt mice. Hematology values measured in EDTA-blood samples.

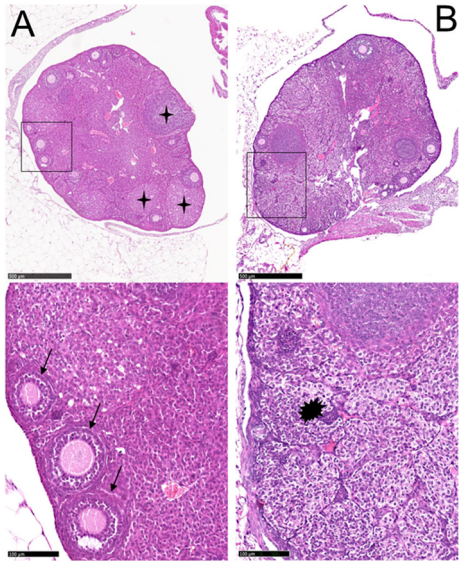

Fig. 8. *Mut*-ko/ki mice exhibit alterations in the ovaries. Ovary from a *Mut*-ki/wt mouse (A): many corpora lutea (+), various stages of follicular development (arrows) and less amounts of interstitial tissue, all compatible with a normally cycling mouse. Ovary from a *Mut*-ko/ki mouse (B): predominance of cords of pale stained hyperplastic interstitial tissue (✹) with fewer follicles. Light micrographs of ovarian tissue stained with hematoxylin and eosin. In the upper panels, black bar represents 500 µm and in the lower panels, it represents 100 µm. All histological examinations were performed on mice at 20 weeks of age.

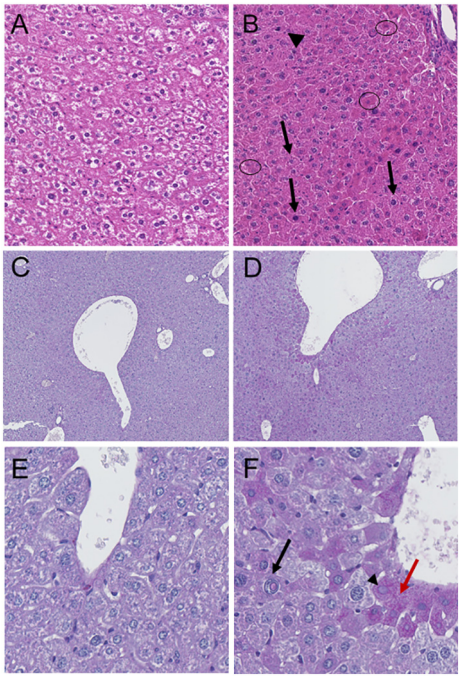

Fig. 9. Histopathological findings in liver. (A), (C) and (E) are representative light micrographs of liver sections from a *Mut*-ki/wt mouse; (B), (D) and (F) are representative from a *Mut*-ko−/ki mouse. All histological examinations were performed on mice at 20 weeks of age. (A) and (B), H&E staining 20× magnification. (A) Shows the normal appearance of the hepatocytes with clear cytoplasm containing glycogen. The nucleus is centrally located, round and contents one or more nucleoli. (B) By comparison, in the liver of a *Mut*-ko−/ki mouse, hepatocytes have condensed dark staining and may be enlarged, show single cell necrosis (marked in circles), high variation in the size of the cell nucleus (anisonucleosis) (arrows) and mitosis (arrowhead). (C–F) PAS staining. (D) The liver of mutant mice shows hepatocellular hypertrophy: consisting of enlarged hepatocytes tinctorially distinct with a diffuse distribution pattern, better seen with lower magnification (10×). (F) The higher magnification (40×) allows visualization of cytoplasm granulation (red arrow) coinciding with an intranuclear inclusion (black arrow), nucleus degeneration (arrowhead) and/or unicellular necrosis. (For interpretation of the references to colour in this figure legend, the reader is referred to the web version of this article.)

end-stage renal disease by adulthood [5]. A similar case is also true for neurological changes. Our model did not display the common neurological signs often described in patients, such as movement disorders and seizures [5]. However, we did identify reduced motor performance, altered thermal sensitivity and changes in anxiety-related behaviour. As with the kidney dysfunction, it is possible that these changes represent mild neurological changes, which either will get worse over time or illustrate differences in disease manifestation between mice and humans. We do note that this is the first evidence of neural dysfunction identified in a model of MMAuria. Altogether, these data validate the clinical relevance of our model. Finally, *Mut*-ko/ki mice exhibited histopathological changes in the liver, such as hepatocellular hypertrophy, granular cytoplasm and formation of body inclusion. This latter might be secondary to an increase in the amount of cytosolic proteins or in the number of organelles such as mitochondria, endoplasmic reticulum or peroxisomes [23]. Liver abnormalities have been reported in MMAuria patients, such as hepatomegaly, histological abnormalities from fibrosis to cirrhosis and enlarged mitochondria accompanied with respiratory chain dysfunction [7,24–27]. More rarely, hepatoblastoma and hepatocellular carcinoma have also been documented in MMAuria [28,29]. Given the dual roles of the liver in metabolite detoxification and energy metabolism, further studies to delineate its role in MMAuria may be invaluable to understanding disease progression.

By comparison with this model on reference chow [13], our new high-protein diet studies reveal, as might be expected, that most measured biochemical and clinical aspects either remain the same or are worsened in severity for mice on the high-protein diet long-term. Long-term growth comparison indicates that *Mut*-ko/ki mice have a much more pronounced failure to thrive when on a high protein diet, especially in the first 50 days of life, while both studies found elevated MMA and C3/C2 levels when mice were on a high-protein diet *versus* a reference diet. However, both with and without a high-protein diet, we

found only small perturbations of electrolyte levels in plasma, indicative of mild early kidney dysfunction, but no histological changes in the kidney. This suggests that even on a high-protein diet *Mut*-ko/ki mice represents a mild model of kidney disease.

4.2. Phenotyping screen reveals rare and potentially new clinical manifestations of disease

In addition to confirming at least mild versions of common clinical disease manifestations, we further identified less common and novel disease symptoms in our mice. This includes decreased iron levels, red blood cells, platelet and plateletcrit, and an increase in mean corpuscular volume. MMAuria patients usually have normal hematology values but neutropenia and pancytopenia were already noted as acute and chronic presentations of the disease [5]. Leukopenia, thrombocytopenia and anemia have also been described in patients [5,7,30,31], whereby anemia has been potentially linked to chronic kidney failure due to an insufficient erythropoietin production. Our results on one hand reflect the thrombocytopenia described in patients with isolated MMAuria and on the other indicate impaired erythropoiesis and macrocytic anemia, which is a typical consequence of complete cobalamin deficiency [32] but not otherwise known in isolated MMAuria.

In addition, *Mut*-ko/ki animals showed alterations in electrocardiography recordings, namely elevated RR and QTc lengths. A prolonged QTc interval causes premature action potentials during the late phases of depolarization and can increase the risk of ventricular arrhythmia or abnormal electrical conduction in the heart. Increased QTc interval, along with cardiomyopathy, is a common and feared manifestation of the related disorder propionic aciduria - a disease due to a defect of propionyl-CoA carboxylase, two enzymatic steps upstream of MUT - and has also been described in MMAuria [5]. Since many of the other disease manifestations are shared between propionic aciduria and MMAuria, it has been hypothesized that alterations in the heart may be secondary due to the accumulation of propionic acid and other metabolites, which are known to be drastically elevated in propionic aciduria and to a lesser degree in MMAuria. Alternatively, these cardiac observations could be secondary to impairments in other organ systems. Further investigation is therefore warranted to confirm the nature of the cardiac defects in this model. Nevertheless, these data highlight the utility of this murine model to bridge the gap from bench to bedside.

In terms of novel findings, we identified decreased bone mineral content and density in *Mut*-ko/ki mice, which could be correlated with the risk of osteopenia and osteoporosis previously described in MMAuria patients [5,8]. It is often discussed whether this risk is iatrogenic in patients receiving a metabolic diet containing low protein, calcium and vitamin D levels [5]. Interestingly, our findings, provided by mutant and control mice given the same high-protein chow, tend to refute this hypothesis. To our knowledge, decreased bone density has not been thoroughly explored in patients so far. However, with the currently increasing life span patients have experienced over the last decades, this may become an important secondary effect later in life and should be monitored. We also found ovarian atrophy, which could be associated with an ovarian follicular insufficiency or impaired regulation of ovarian folliculogenesis. In mice, ovarian atrophy typically represents an age-related change (*e.g.* > 1 year old) but when it occurs prematurely (20 weeks old) it represents an aberrant state [33]. Although *MUT* is known to be moderately expressed at the mRNA and protein levels in ovarian tissue in humans (The Human Protein Atlas, https://www.proteinatlas.org/) and mice [34], this is to our knowledge the first time that ovaries have been investigated in MMAuria. This suggests that the observed alterations might be caused by an impaired follicular reserve in *Mut*-ko/ki females. This may be consistent with the premature menopause reported in a 36-year-old female patient with MMAuria and a 45-year-old female patient suffering from propionic aciduria [35,36]. Again, in light of the better clinical management in current times, having children may be an option for some patients in the near future. In this case, it will be interesting to identify whether their ability to do so is affected, and if so, how they can best be supported.

5. Conclusions

In sum, we optimized a bespoke mouse model of MMAuria, and by performing a broad phenotypic screen not only identified common clinical manifestations of the disease, but also novel presentations. It will be important to determine whether these latter are truly applicable to humans or possibly due to the divergence between human and mouse biology. We suggest attention should be paid to decreased cardiac function, bone mineral density especially in aging patients, for signs of liver damage in both sexes and reproductive capacity in females.

So far, the treatments that have been attempted in MMAuria mouse models were assessed by investigating individual biomarkers only, thus limiting their clinical assessment. In this study, we identified quantifiable readouts, such as body weight, bone mineral density and content, hypoactivity in the acute setting, plasma electrolyte levels, QTc, and number of follicles. Once confirmed and studied in patients, these readouts would enable a comprehensive clinical output that could be used to assess the efficacy of potential novel therapeutic avenues, such as gene or mRNA therapy. Finally, many of the symptoms identified in these mice are likely related to metabolic alterations affecting energy. A more in-depth study of these changes may provide an exciting opportunity to elucidate further pathophysiological mechanisms of the disease.

Transparency document

The Transparency document associated with this article can be found, in online version.

Acknowledgments

This work was supported by the Rare Disease Initiative Zurich (radiz), a clinical research priority program for rare diseases of the University of Zurich (to M.L., D.S.F. and M.R.B.); the Swiss National Science Foundation Grant [SNSF 31003A_175779] (to M.R.B.); the Wolferman Nägeli Foundation (to M.R.B.) and by the German Federal Ministry of Education and Research [Infrafrontier grant 01KX1012] (to MHdA) and to the German Center for Diabetes Research (DZD e.V.) (to MHdA). The authors declare that they have no conflicts of interest with the contents of this article.

We thank Michelle Daniel (University of Zurich) for statistical advice and GMC technicians and animal caretakers for expert technical support.

Appendix A. Supplementary data

Supplementary data to this article can be found online at https://doi.org/10.1016/j.bbadis.2019.165622.

References

[1] W.A. Fenton, R.A. Gravel, D.S. Rosenblatt, Disorders of propionate and methylmalonate metabolism, in: D. Valle, A. Beaudet, B. Vogelstein, K.W. Kinzler, S.E. Antonarakis, A. Ballabio, M. Gibson, G. Mitchell (Eds.), The Online Metabolic and Molecular Bases of Inherited Disease, online edi McGraw-Hill, 2014.

[2] B. Fowler, J.V. Leonard, M.R. Baumgartner, Causes of and diagnostic approach to methylmalonic acidurias, J. Inherit. Metab. Dis. 31 (2008) 350–360.

[3] J. Janata, N. Kogekar, W.A. Fenton, Expression and kinetic characterization of methylmalonyl-CoA mutase from patients with the mut-phenotype: evidence for naturally occurring interallelic complementation, Hum. Mol. Genet. 6 (9) (1997) 1457–1464.

[4] F. Hörster, M.R. Baumgartner, C. Viardot, T. Suormala, P. Burgard, B. Fowler, G.F. Hoffmann, S.F. Garbade, S. Kölker, E.R. Baumgartner, Long-term outcome in methylmalonic acidurias is influenced by the underlying defect (mut0, Mut-, cblA, cblB), Pediatr. Res. 62 (2) (2007) 225–230.

[5] M.R. Baumgartner, F. Hörster, C. Dionisi-Vici, G. Haliloglu, D. Karall, K.A. Chapman, M. Huemer, M. Hochuli, M. Assoun, D. Ballhausen, A. Burlina, B. Fowler, S.C. Grünert, S. Grünewald, T. Honzik, B. Merinero, C. Pérez-Cerdá, S. Scholl-Bürgi, F. Skovby, F. Wijburg, A. MacDonald, D. Martinelli, J.O. Sass, V. Valayannopoulos, A. Chakrapani, Proposed guidelines for the diagnosis and management of methylmalonic and propionic acidemia, Orphanet J. Rare Dis. 9 (1) (2014) 1–36.

[6] Y.P. Ktena, S.M. Paul, N.S. Hauser, J.L. Sloan, A. Gropman, I. Manoli, C.P. Venditti, Delineating the spectrum of impairments, disabilities, and rehabilitation needs in methylmalonic acidemia (MMA), Am. J. Med. Genet. A 167 (9) (2015) 2075–2084.

[7] I. Manoli, J.L. Sloan, C.P. Venditti, Isolated methylmalonic acidemia, Gene Reviews, 2005.

[8] J.L. Fraser, C.P. Venditti, Methylmalonic and propionic acidemias: clinical management update, Curr. Opin. Pediatr. 28 (6) (2016) 682–693.

[9] H. Peters, M. Nefedov, J. Sarsero, J. Pitt, K.J. Fowler, S. Gazeas, S.G. Kahler, P.A. Ioannou, A Knock-out mouse model for methylmalonic aciduria resulting in neonatal lethality, J. Biol. Chem. 278 (2003) 52909–52913.

[10] R.J. Chandler, J. Sloan, H. Fu, M. Tsai, S. Stabler, R. Allen, K.H. Kaestner, H.H. Kazazian, C.P. Venditti, Metabolic phenotype of methylmalonic acidemia in mice and humans: the role of skeletal muscle, BMC Med. Genet. 8 (2007) 64.

[11] J. Sénac, R. Chandler, J. Sysol, L. Li, C. Venditti, Gene therapy in a murine model of methylmalonic acidemia using rAAV9-mediated gene delivery, Gene Ther. 19 (2011) 385–391.

[12] I. Manoli, J.R. Sysol, L. Li, P. Houillier, C. Garone, C. Wang, P.M. Zerfas, K. Cusmano-Ozog, S. Young, N.S. Trivedi, J. Cheng, J.L. Sloan, R.J. Chandler, M. Abu-Asab, M. Tsokos, A.G. Elkahloun, S. Rosen, G.M. Enns, G.T. Berry, V. Hoffmann, S. Dimauro, J. Schnermann, C.P. Venditti, Targeting proximal tubule mitochondrial dysfunction attenuates the renal disease of methylmalonic acidemia, PNAS 110 (33) (2013) 13552–13557.

[13] P. Forny, A. Schumann, M. Mustedanagic, D. Mathis, M.A. Wulf, N. Nägele, C.D. Langhans, A. Zhakupova, J. Heeren, L. Scheja, R. Fingerhut, H.L. Peters, T. Hornemann, B. Thony, S. Kölker, P. Burda, D.S. Froese, O. Devuyst, M.R. Baumgartner, Novel mouse models of methylmalonic aciduria recapitulate phenotypic traits with a genetic dosage effect, J. Biol. Chem. 291 (2016) 20563–20573.

[14] P. Forny, D.S. Froese, T. Suormala, W.W. Yue, M.R. Baumgartner, Functional characterization and categorization of missense mutations that cause methylmalonyl-coA mutase (MUT) deficiency, Hum. Mutat. 35 (2014) 1449–1458.

[15] V. Gailus-Durner, H. Fuchs, L. Becker, I. Bolle, M. Brielmeier, J. Calzada-Wack, R. Elvert, N. Ehrhardt, C. Dalke, T.J. Franz, E. Grundner-Culemann, S. Hammelbacher, S.M. Hölter, G. Hölzlwimmer, M. Horsch, A. Javaheri, S. Vetoslav Kalaydjiev, M. Klempt, E. Kling, S. Kunder, C. Lengger, T. Lisse, T. Mijalski, B. Naton, V. Pedersen, C. Prehn, G. Przemeck, I. Racz, C. Reinhard, P. Reitmeir, I. Schneider, A. Schrewe, R. Steinkamp, C. Zybill, J. Adamski, J. Beckers, H. Behrendt, J. Favor, J. Graw, G. Heldmaier, H. Höfler, B. Ivandic, H. Katus, P. Kirchhof, M. Klingenspor, T. Klopstock, A. Lengeling, W. Müller, F. Ohl, M. Ollert, L. Quintanilla-Martinez, J. Schmidt, H. Schulz, E. Wolf, W. Wurst, A. Zimmer, D.H. Busch, M.H. de Angelis, Introducing the German Mouse Clinic: open access platform for standardized phenotyping, Nat. Methods 2 (6) (2005) 403–404.

[16] H. Fuchs, J.A. Aguilar-Pimentel, O.V. Amarie, L. Becker, J. Calzada-Wack, Y.L. Cho, L. Garrett, S.M. Hölter, M. Irmler, M. Kistler, M. Kraiger, P. Mayer-Kuckuk, K. Moreth, B. Rathkolb, J. Rozman, P. da Silva Buttkus, I. Treise, A. Zimprich, K. Gampe, C. Hutterer, C. Stöger, S. Leuchtenberger, H. Maier, M. Miller, A. Scheideler, M. Wu, J. Beckers, R. Bekeredjian, M. Brielmeier, D.H. Busch, M. Klingenspor, T. Klopstock, M. Ollert, C. Schmidt-Weber, T. Stöger, E. Wolf, W. Wurst, A. Yildirim, A. Zimmer, V. Gailus-Durner, M. Hrabě de Angelis, Understanding gene functions and disease mechanisms: Phenotyping pipelines in the German Mouse Clinic, Behav. Brain Res. 352 (2018) 187–196.

[17] H. Fuchs, V. Gailus-Durner, T. Adler, J.A. Aguilar-Pimentel, L. Becker, J. Calzada-Wack, P. Da Silva-Buttkus, F. Neff, A. Götz, W. Hans, S.M. Hölter, M. Horsch, G. Kastenmüller, E. Kemter, C. Lengger, H. Maier, M. Matloka, G. Möller, B. Naton, C. Prehn, O. Puk, I. Rácz, B. Rathkolb, W. Römisch-Margl, J. Rozman, R. Wang-Sattler, A. Schrewe, C. Stöger, M. Tost, J. Adamski, B. Aigner, J. Beckers, H. Behrendt, D.H. Busch, I. Esposito, J. Graw, T. Illig, B. Ivandic, M. Klingenspor, T. Klopstock, E. Kremmer, M. Mempel, S. Neschen, M. Ollert, H. Schulz, K. Suhre, E. Wolf, W. Wurst, A. Zimmer, M. Hrabě de Angelis, Mouse phenotyping, Methods, 2011.

[18] J. Rathkolb B, W. Hans, C. Prehn, H. Fuchs, V. Gailus-Durner, B. Aigner, M. Adamski, E. Wolf, Hrabe de Angelis, Clinical chemistry and other laboratory tests on mouse plasma or serum, Curr. Protoc. Mouse Biol. 3 (2) (2013) 69–100.

[19] S.M. G-Holter, L. Garrett, J. Einicke, B. Sperling, P. Dirscherl, A. Zimprich, H. Fuchs, V. W Durner, M. Hrabe de Angelis, Wurst, Assessing Cognition in Mice, Curr. Protoc. Mouse Biol. 5 (4) (2015) 331–358.

[20] R.L. Batterham, H. Heffron, S. Kapoor, J.E. Chivers, K. Chandarana, H. Herzog, C.W. Le Roux, E.L. Thomas, J.D. Bell, D.J. Withers, Critical role for peptide YY in protein-mediated satiation and body-weight regulation, Cell Metab. 4 (2006) 223–233.

[21] The Eumorphia Consortium, EMPReSS: standardized phenotype screens for functional annotation of the mouse genome, Nat. Genet. 37 (11) (2005) 1155.

[22] C.T. Turgeon, M.J. Magera, C.D. Cuthbert, P.R. Loken, D.K. Gavrilov, S. Tortorelli, K.M. Raymond, D. Oglesbee, P. Rinaldo, D. Matern, Determination of total homocysteine, methylmalonic acid, and 2-methylcitric acid in dried blood spots by tandem mass spectrometry, Clin. Chem. 56 (11) (2010) 1686–1695.

[23] B. Thoolen, R.R. Maronpot, T. Harada, A. Nyska, C. Rousseaux, T. Nolte, D.E. Malarkey, W. Kaufmann, K. Küttler, U. Deschl, D. Nakae, R. Gregson, M.P. Vinlove, A.E. Brix, B. Singh, F. Belpoggi, J.M. Ward, Proliferative and non-proliferative lesions of the rat and mouse hepatobiliary system, Toxicol. Pathol. 37 (2010) 1155.

[24] A. Imbard, N. Garcia Segarra, M. Tardieu, P. Broué, J. Bouchereau, S. Pichard, H.O. de Baulny, A. Slama, C. Mussini, G. Touati, M. Danjoux, P. Gaignard, H. Vogel, F. Labarthe, M. Schiff, J.F. Benoist, Long-term liver disease in methylmalonic and propionic acidemias, Mol. Genet. Metab. 123 (4) (Apr. 2018) 433–440.

[25] R.J. Chandler, P.M. Zerfas, S. Shanske, J. Sloan, V. Hoffmann, S. DiMauro, C.P. Venditti, Mitochondrial dysfunction in mut methylmalonic acidemia, FASEB J. 7 (2009) 63–66.

[26] P. Karimzadeh, N. Jafari, F. Ahmad Abadi, S. Jabbedari, M.M. Taghdiri, H. Nemati, S. Saket, S.F. Shariatmadari, M.R. Alaee, M. Ghofrani, S.H. Tonekaboni, Methylmalonic acidemia: diagnosis and neuroimaging findings of this neurometabolic disorder (an iranian pediatric case series), Iran. J. Child Neurol. 7 (3) (2013) 63–66.

[27] Y. De Keyzer, V. Valayannopoulos, J.-F. Benoist, F. Batteux, F. Lacaille, L. Hubert, D. Chrétien, B. Chadefeaux-Vekemans, P. Niaudet, G. Touati, A. Munnich, P. De Lonlay, Multiple OXPHOS deficiency in the liver, kidney, heart, and skeletal muscle of patients with methylmalonic aciduria and propionic aciduria, Pediatr. Res. 66 (1) (2009) 91–95.

[28] M.A. Cosson, G. Touati, F. Lacaille, V. Valayannnopoulos, C. Guyot, G. Guest, V. Verkarre, D. Chrétien, D. Rabier, A. Munnich, J.F. Benoist, Y. de Keyzer, P. Niaudet, P. de Lonlay, Liver hepatoblastoma and multiple OXPHOS deficiency in the follow-up of a patient with methylmalonic aciduria, Mol. Genet. Metab. 95 (1–2) (Sep. 2008) 107–109.

[29] P. Forny, M. Hochuli, Y. Rahman, M. Deheragoda, A. Weber, J. Baruteau, S. Grunewald, Liver neoplasms in methylmalonic aciduria: an emerging complication, J. Inherit. Metab. Dis. (Jul. 2019) jimd.12143.

[30] I. Manoli, J.L. Sloan, C.P. Venditti, Isolated Methylmalonic Acidemia, GeneReviews®, 2005.

[31] N.A. Bakshi, T. Al-Anzi, | Said, Y. Mohamed, | Zuhair Rahbeeni, M. Alsayed, M. Al-Owain, R.A. Sulaiman, Spectrum of Bone Marrow Pathology and Hematological Abnormalities in Methylmalonic Acidemia; Spectrum of Bone Marrow Pathology and Hematological Abnormalities in Methylmalonic Acidemia, (2018).

[32] R. Green, Vitamin B12 deficiency from the perspective of a practicing hematologist, Blood. 129 (2017) 2603–2611.

[33] R.R. Maronpot, G.A. Boorman, B.W. Gaul, B.M. Wagner, E. Research Professor of Pathology, T. Takeuchi, K.E. Fukuoka, E. Professor of Pathology, R.R. Maronpot, G.A. Boorman, B.W. Gaul (Eds.), Book Reviews: Pathology of the Mouse, Reference and Atlas, Cache River Press, Vienna, Illinois, 1999(699 pp," Cache River Press, 1999).

[34] M.F. Wilkemeyer, E.R. Andrews, F.D. Ledley, Genomic structure of murine methylmalonyl-CoA mutase: evidence for genetic and epigenetic mechanisms determining enzyme activity, Biochem. J. 296 (Pt 3) (1993) 663–670.

[35] M.D. Bain, J. Till, M.G. Jones, G.T.N. Besley, P. Lee, D. Oliveira, R.A. Chalmers, Methylmalonic aciduria: follow-up and enzymology on the original case after 36 years, J. Inherit. Metab. Dis. 28 (6) (Dec. 2005) 1179–1180.

[36] C. Lam, L.R. Desviat, C. Perez-Cerdá, M. Ugarte, B.A. Barshop, S. Cederbaum, 45-Year-Old Female with Propionic Acidemia, Renal Failure, and Premature Ovarian Failure; Late Complications of Propionic Acidemia? (2011).